JSHC
Japan Society of Histochemistry and Cytochemistry
Established 1959

Acta Histochem. Cytochem. 42 (3): 65–71, 2009
doi:10.1267/ahc.09009

Histochemical Analysis of Renal Dysplasia with Ureteral Atresia

Toyoko Kawate[1], Ryuki Kawamura[3], Takenori Uchida[3], Kyosuke Takahashi[3], Tomohiro Hasegawa[3], Haruo Futamata[1], Ryohei Katoh[2] and Sen Takeda[1]

[1]Department of Anatomy and Cell Biology, The University of Yamanashi Interdisciplinary Graduate School of Medicine, [2]Department of Human Pathology, The University of Yamanashi Interdisciplinary Graduate School of Medicine and Engineering and [3]The University of Yamanashi Faculty of Medicine, 1110 Shimo-Kateau, Chuo, Yamanashi 409–3898, Japan

Received March 11, 2009; accepted March 23, 2009; published online April 25, 2009

Unilateral small kidney with ureteral obstruction was discovered in a 74-year-old female cadaver during an anatomical dissection course. In order to elucidate the histogenesis of renal dysplasia, we carried out histochemical and immunohistochemical analyses. On macroscopic view, the kidney was approximately 3 cm in length, 2 cm in width and weighed only 9 g. Although the ureter ran from the renal hilus to the bladder, its width was under 2 mm. The renal parenchyma was extremely thin and there was a large congested vein in the renal sinus. On microscopic examination of the kidney, we observed that numerous developing renal tubules had cytokeratin-positive epithelia, most of which were surrounded by concentric fibrosis. However, we could not detect any structures resembling the collecting duct, renal tubules, renal pelvis, or glomeruli. The concentric mesencymal fibrous tissue surrounding the immature renal tubules contained the smooth muscles that were positive for h-caldesmon. Serial sections of the ureter revealed several small and discontinuous lacunae lined by cuboidal and transitional epithelium, which did not constitute a patent lumen through the bladder. This case is a rare case of renal dysplasia with defect in recanalization of the ureteral bud during the early developmental stage.

Key words: kidney, ureter, renal dysplasia, caldesmone, immunohistochemistry

I. Introduction

Unilateral small kidney comprises any of the following morphological characteristics: the kidney is less than half the size of a normal kidney; the renal parenchyma occupies less than one-third of the renal mass; or the kidney contains no more than five renal papillae [19]. Generally, the etiology of small kidney is either due to congenital hypoplasia or dysplasia (primary), possibly due to developmental failure, or is secondary to conditions of chronic kidney disease such as recurrent pyelonephritis, ischemic events, vesico-ureteral reflux (VUR) or long-lasting renal dialysis. In progressive chronic kidney diseases (CKD), an augmentation of the interstitial extracellular matrix (ECK), which results from the transition of renal tubular epithelium to mesenchyme (epithelial to mesenchymal trasition, EMT), is suggested to be responsible for secondary parenchymal atrophy, which results in small kidney [4]. Interestingly, EMT is believed to be important for both the embryonic renal development [5] as well as for the pathogenesis of CKD. In these cases, myofibroblasts with α-smooth muscle actin (αSMA) have been detected [15].

Congenital (primary) small kidney frequently accompanies urinary tract anomalies such as ureteral atresia and obstruction in early stage of development. The ureteral bud forming the ureter originates from the mesonephric duct (Wolffian duct). Although the phenomena of fetal ureteral obstruction and recanalization had been already reported in 1894 [21], Ruano-Gill *et al.* [18] conducted a detailed observation in human embryos and fetuses. Furthermore, Alcaraz *et al.* [2] conducted the ultrastructural analysis on the embryonic ureteral obstruction and recanalization in human and rat. After that, the interaction between uretral buds and metanephric blastema in turn induces the matura-

Correspondence to: Sen Takeda, Department of Anatomy and Cell Biology, The University of Yamanashi Interdisciplinary Graduate School of Medicine, 1110 Shimo-Kateau, Chuo, Yamanashi 409–3898, Japan. E-mail: stakeda@yamanashi.ac.jp

Table 1. *Antibodies used for immunohistochemistry*

Antibody (clone)	Antigen	Source of antibody	Dilution
34bE12	human pan-cytokeratin (high molecular weight, 48–67 kD, 1, 5, 10, 14)	Dako (Glostrup, Denmark)	1:100
1A4	human smooth muscle actin (αSMA)	Sigma (St. Louis, MO, USA)	1:100
h-CD	human caldesmon	Dako (Glostrup, Denmark)	1:50

tion of nephrons. Renal glomeruli develop around 58 days after implantation. Therefore, ureteral development has a great effect on the pathogenesis of congenital kidney diseases.

Concerning the congenital kidney malformations, the following three categories are well-recognized: agenesis, hypoplasia (reduced kidney size with a small number of nephrons), and dysplasia [20]. The classic categorization by Potter [17] is widely adopted, but it was based on microscopic findings, especially in terms of early growth inhibition of metanephric blastema. A more complicated classification proposed by Itatani *et al.* [7] comprised agenesis (both tubules and glomeruli are absent), dysgenesis (primitive tubules without glomeruli), dysplasia (matured primitive tubules with primitive glomeruli), and hypoplasia (a small number of matured tubules with glomerul) with or without cysts. Although we identified many abnormal tubules as well as mesenchymal cells and smooth muscles by using immunohistochemical methods, we did not find either glomeruli or matured tubular structures in the affected kidney. Taking these findings and criteria of classification into account, we propose that the present case can be diagnosed as unilateral renal dysplasia with highly dysplastic histology, accompanied with the ureteral atresia.

II. Materials and Methods

Unilateral small kidney with ureteral obstruction was discovered in a 74-year-old female cadaver during an anatomical dissection course in 2007. The subject had been diagnosed with diabetes mellitus (DM), diabetic nephropathy and arteriosclerosis obliterans (ASO) for over a decade. In addition, she had a history of renal blood dialysis for 13 years before she died. To elucidate the etiology of the small kidney and the ureter, we performed macroscopic observation and histochemical and immunohistochemical analysis. Concerning the usage of human samples for this study, we obtained official approval from the donor in advance.

Histochemistry

For histological analysis, we used HE, PAS, Masson-Trichrome and Elastica van Gieson staining of formalin-fixed, paraffin-embedded specimens of the both kidneys and the ureters from the cadaver. In order to confirm whether or not the lacunae in the ureter were continuous to form a single lumen, we carried out serial longitudinal and transverse sections on the proximal, middle and distal part of ureter (each containing 36 sections from 600 μm length). Each section was observed under light microscope (BX50, Olympus, Tokyo, Japan) and the images were captured and stored using CCD camera system (VB7010, Keyence, Osaka, Japan). All images were modified using Adobe Photoshop CS3 (Adobe Systems Inc., San Jose, CA). The images from serial sections were traced with pen tablet (CTE-450/S0, WACOM, Otone, Japan) and stacked using Adobe Photoshop.

Immunohistochemistry

Formalin-fixed, paraffin-embedded specimens were used for immunohistochemical analysis with a panel of antibodies (Table 1). Briefly, sections were subjected to autoclave for antigen retrieval in citric acid buffer at pH 6.0 for 10 min at 121°C. Endogenous peroxidase was blocked with 3% H_2O_2 in methanol for 5 min. After washing with phosphate-buffered saline (PBS) at pH 7.4, the sections were incubated with the primary monoclonal antibodies (Table 1) in PBS supplemented with1% BSA for 60 min at room temperature (RT). After washing with PBS, sections were incubated with horse radish peroxidase (HRP)-conjugated secondary antibodies in 1% BSA-PBS for 30 min at RT. After washing with PBS, immunoreactive products on sections were visualized by reacting with 3,3'-diaminobenzidine 4HCl (DAB) in the presence of 3% H_2O_2. Microscopic observations were examined as described above.

III. Results

On macroscopic inspection, the location of both kidneys and ureters were almost normal. However, the left kidney was extremely small, measuring approximately 3 cm in length and 2 cm in width, and weighing only 9 g (Fig. 1A). The surface of the renal capsule appeared irregular (Fig. 1A). Though the renal vein appeared to be slightly narrower than normal, the renal artery was very thin (2 mm in diameter, Fig. 1A and B). At a point 5 mm distal from the aorta, the renal artery bifurcated (upper and lower branch) (Fig. 1B), and the upper branch reached the superior part of the kidney, where it gave rise to two inferior suprarenal arteries and a thin upper renal artery. The lower branch entered into the kidney via the renal hilus. On a frontal section, it was noted that the large varicose vein in the renal sinus was filled with coagulated blood (Fig. 1C). In addition, the renal parenchyma was very hypoplastic, leaving no trace of calyces nor pelvis (Fig. 1D).

Histological examination of the left kidney revealed several important findings: (1) an absence of the typical

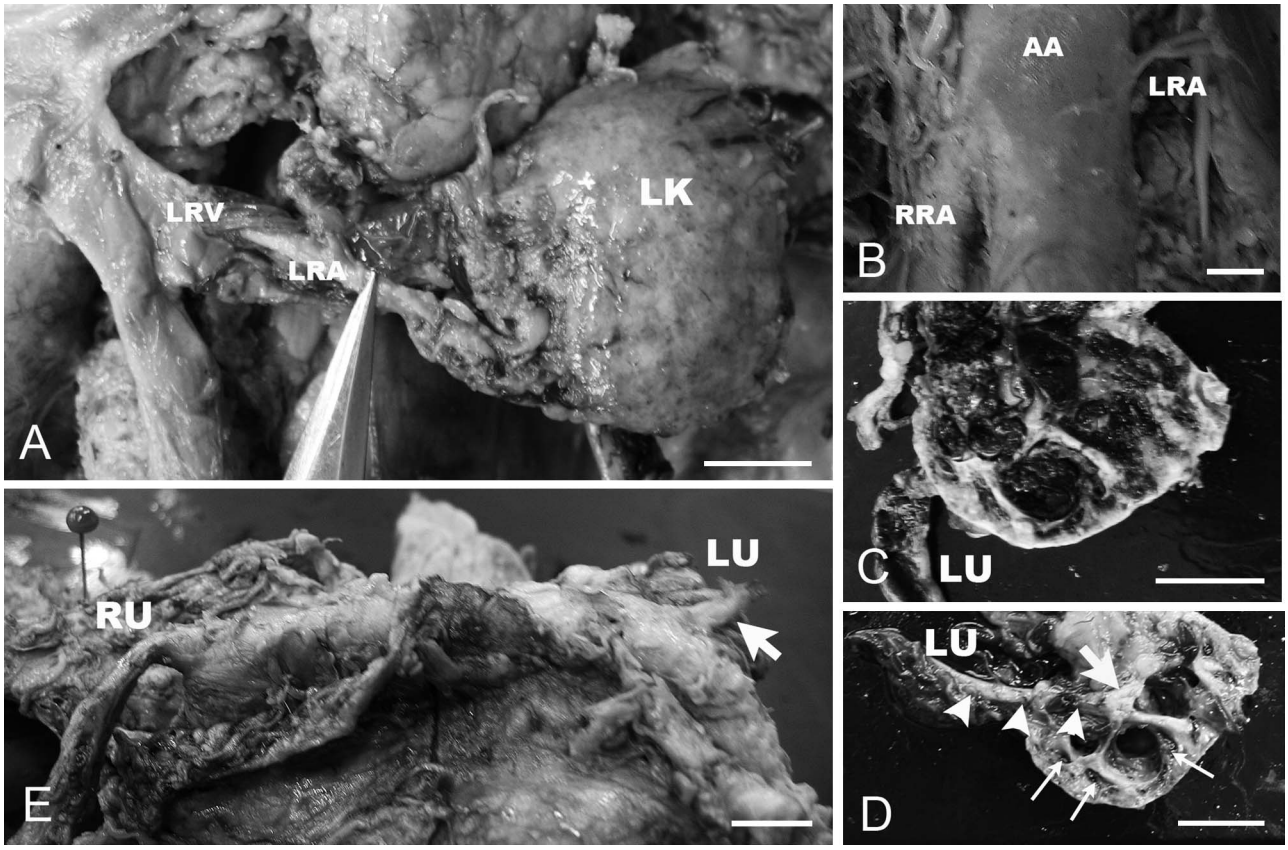

Fig. 1. Macroscopic images of the renal dysplasia in the left kidney. **A**) The left kidney (LK) was very small and showed an irregular surface. Both the renal vein and the thin renal artery (held by a pair of tweezers in the center of the panel) were identified. **B**) The left renal artery was much thinner than the right renal artery. **C**) On the transected surface of the kidney, the extremely enlarged varicosities of vein were filled with coagulated blood, which also filled the renal sinus. The renal parenchyma was severely hypoplastic, so that the cortex and medulla were not clearly demarcated. **D**) After washing out the coagulated blood, the course of the ureter was visualized by arrowheads, which led to the rudimentary renal pelvis (arrow). Small arrows show arcuate veins. **E**) The site of left vesico-ureteral confluence was incomplete when compared with that of the right side. The left ureter was much thinner compared with the right one (arrow). Bars=1 cm. LK, left kidney; LRV, left renal vein; LRA, left renal artery; RRA, right renal artery; LU, left ureter; RU, right ureter; AA, abdominal aorta.

collecting duct, renal glomeruli, calyces and pelvis; and (2) two types of lacunae lined with cuboidal or lucent columnar epithelium. Some immature tubules were surrounded by the mesenchymal proliferation (arrows in Fig. 2A), whereas the other pleomorphic lacunae lined with either cuboidal or squamous epithelium contained hyaline-like materials in their lumen (arrowheads in Fig. 2A). The lacunae lined with the lucent columnar epithelium mimicked the immature collecting duct (Fig. 2A, B, D, F), which tended to be located in the deeper layers of the affected kidney. These lacunae were frequently arranged in a tandem manner and occasionally gave rise to bifurcation at their end (Fig. 2A and B). Furthermore, the lucent columnar epithelium was surrounded by concentric proliferation of fibrous tissue and smooth muscle cells, which was revealed by Elastica van Gieson staining (Fig. 2B), and anti-h-caldesmon antibody (Fig. 2E). Anti-αSMA antibody showed the existence of myofibroblasts as evidence for EMT (Fig. 2C and D).

The pleomorphic lacunae (Fig. 2G) showed no features of renal tubules (Fig. 2A, C, E and G). However, we could find some aggregation of immature cells obliterating the lacuna. These cells were not stained by anti-cytokeratin antibody (arrow in Fig. 2H). Moreover, some of these tubules tended to show extreme dilatation (>100 μm in diameter). Their lacunae were filled with hyaline-like materials (Fig. 2A) that were positive for PAS staining (not shown). The interstitium around the tubules showed mild proliferation of mesenchyme with lesser content of smooth muscle compared with the status described above (Fig. 2C and E). Several clusters of immature epithelial cells did not display cytokeratin-immunopositivity (Fig. 2H).

The left ureter was extremely thin (<2 mm in diameter) (Fig. 1A, D) but reached the bladder (Fig. 1E arrow). However, the macroscopic findings of the left ureter connecting to the bladder appeared to be different from that of right one (Fig. 1C). The left ureter did not *bona fide* traverse the bladder wall and the ureteral lumen was not patent to the bladder. Moreover, the left border of the trigonum vesicae was quite ambiguous. On histological inspection, the ureter *per se* contained a layer of smooth

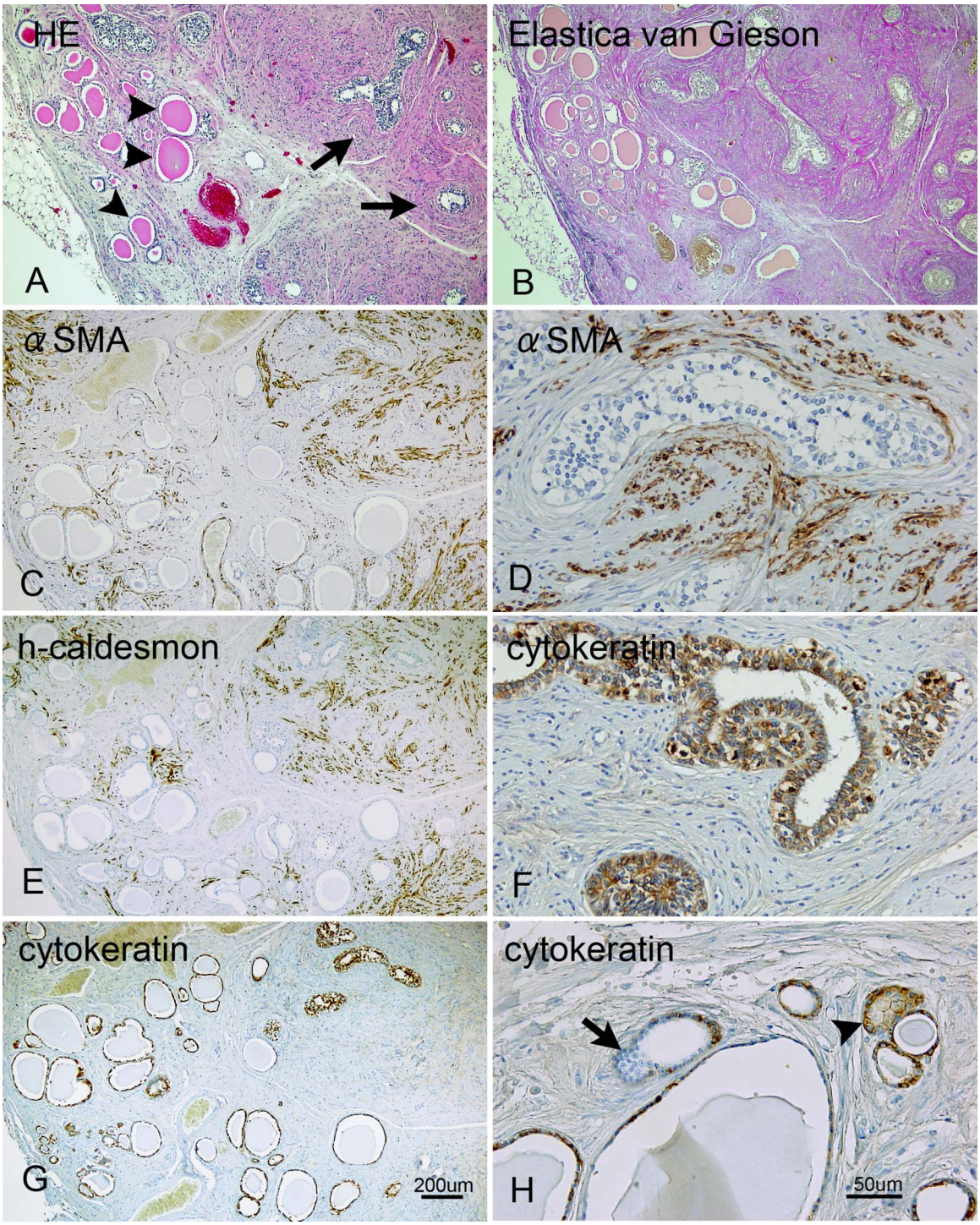

Fig. 2. Histopathological and immunohistochemical observation of the left kidney (dysplastic side). **A**) Hematoxylin-eosin (HE) staining. In this panel, no specific structure corresponding to the renal glomeruli, calyces and pelvis were identified. **B**) Elastica von Gieson staining. Immature tubules lined with lucent cuboidal epithelium (stained with a yellowish color) existed in the middle of concentric proliferation of fibrous tissues (stained with a reddish color) and smooth muscle cells (stained with a yellowish color). **C** and **D**) Localization of smooth muscle cells stained with anti-αSMA antibody. αSMA-immunoreactivity (stained in brownish color) was present in the fibrous tissue surrounding the immature tubules lined with lucent cuboidal or columnar epithelium, as observed in **C**. **D**) Enlarged image of the tissue in **C**. **F, G** and **H**) Renal tissue stained with the anti-cytokeratin antibody. **E**) Anti-h-caldesmon staining of renal tissue revealed scattered parenchymal pattern mimicking that of αSMA-immunoreactivity. **F**) The cuboidal or columnar epithelia surrounded by the concentric fibrous tissues were immunopositive for cytokeratin (stained in brownish color). **G**) Cytokeratin-immunoreactivity was also localized to the flat or cuboidal epithelia lining the cysts in the relatively superficial layer of the parenchyma. **H**) Occasionally, several clusters of immature epithelial cells did not display cytokeratin-immunopositivity (arrow). Some cytokeratin-positive epithelial cells proliferated to fill the lumen (arrowhead). Bar for **A–C, E** and **G**=200 μm; bar for **D, F** and **H**=50 μm.

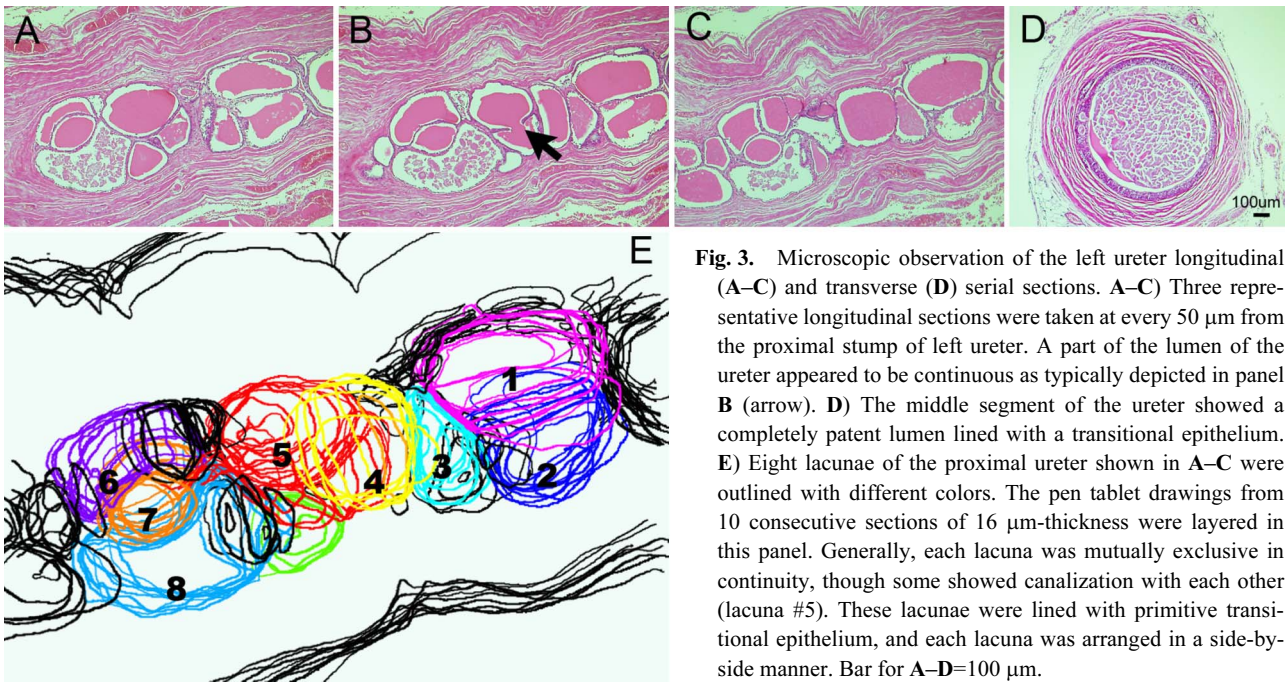

Fig. 3. Microscopic observation of the left ureter longitudinal (**A–C**) and transverse (**D**) serial sections. **A–C**) Three representative longitudinal sections were taken at every 50 μm from the proximal stump of left ureter. A part of the lumen of the ureter appeared to be continuous as typically depicted in panel **B** (arrow). **D**) The middle segment of the ureter showed a completely patent lumen lined with a transitional epithelium. **E**) Eight lacunae of the proximal ureter shown in **A–C** were outlined with different colors. The pen tablet drawings from 10 consecutive sections of 16 μm-thickness were layered in this panel. Generally, each lacuna was mutually exclusive in continuity, though some showed canalization with each other (lacuna #5). These lacunae were lined with primitive transitional epithelium, and each lacuna was arranged in a side-by-side manner. Bar for **A–D**=100 μm.

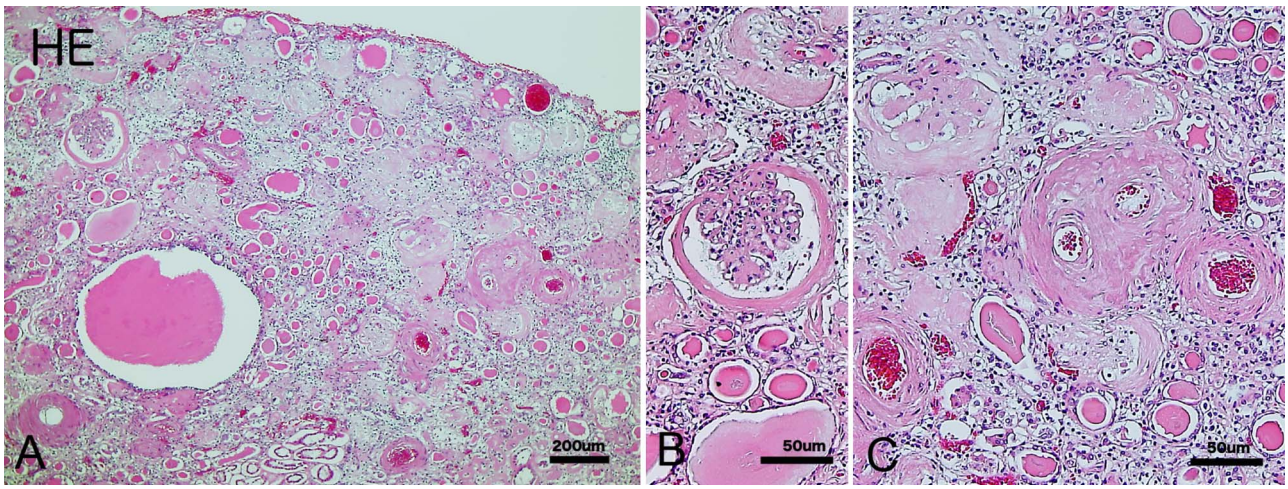

Fig. 4. The renal cortex of the right kidney. **A–C**) The histogenesis of the right kidney appeared to be normal. However, it displayed pathological changes typical of diabetic kidneys, such as nodular glomerulonephritis and deposition of hyaline-like material in the glomeruli, which had an appearance similar to the thyroid gland. The renal vessels are surrounded by marked fibers, with an "onion skin"-like pattern. Bar for **A**=200 μm, **B,C**=50 μm.

muscle and the lacunae-like structures were lined with cuboidal or transitional epithelium (Fig. 3A–D). In order to elucidate whether or not the lacunae were continuous to form a single lumen, we carried out serial longitudinal and transverse sections on the proximal, middle and distal part of the ureter. Most of the lacunae in the proximal- and distal-ureter were discontinuous, though some of them showed continuity (Fig. 3B). Tracing of serial sections also revealed discontinuous lacunae in most cases (e.g. #4 and 5 in Fig. 3E). On the contrary, in the middle part, the lacunae were completely continuous to form one large lumen spanning for over 600 μm, whose lining was the transitional epithelium (Fig. 3D). The smooth muscle layer appeared to be normal (Fig. 3A–D).

The right kidney showed an irregular surface suggesting the formation of small cysts in the renal parenchyma, although it weighed approximately 120 g. Histological examination revealed pathological changes typical of the diabetic kidney, such as a thyroid-like appearance, nodular lesions indicating glomerulonephritis, and the deposition of hyaline-like material in the glomeruli (Fig. 4A, B). However, the histogenesis of the right kidney appeared to be normal.

We did not identify fibrosis of the renal parenchyma, as observed in the contralateral side, except for the renal vessels on the right side of the kidney, where there was marked perivascular fibrosis of the renal vessels, with an "onion skin"-like appearance (Fig. 4C).

IV. Discussion

Herein we identified a unilateral renal dysplasia with ureteral atresia. This case was completely devoid of renal glomeruli, suggesting the incomplete development of the nephrons. Furthermore, the renal tissue contained many various-sized developing renal tubules, which were similar to those reported in previous studies [3, 22]. In addition, immunohistochemical staining of these structures with anti-cytokeratin and anti-h-caldesmon antibodies revealed epithelial cells surrounded by smooth muscle cells. Also, the left ureter had many lacunae lined with a single- to multi-layered epithelia surrounded by muscle layers.

The major concern in this case is whether or not the etiology of renal dysplasia is primary developmental defects, because this cadaver had suffered from systemic diseases such as DM and ASO and had been treated with hemodialysis for 13 years. An end-stage kidney resulting from a long-term hemodialysis is reported to share several characteristics observed herein. The degree of reduction in kidney size was average to 78.2 g [13]. On histological examination, the diabetic end-stage kidney frequently shows glomeruli and renal tubules mimicking some stages of embryonic hyperplasia, such as atrophy or dilation denominated as thyroid appearance. Mesenchymal proliferation with increased expression of smooth muscle also developed [4]. Furthermore, thickening of smooth muscle layer surrounding the arteries and veins was also noted. Tubulovenous thrombosis was found in veins [6, 14]. On this account, the right kidney of the present case exactly displayed the condition of end-stage kidney. However, the macroscopic and histological findings of the left kidney suggested the possibility of congenital developmental failure. We assume the following points for supporting our hypothesis: 1) the size of the affected kidney was significantly small and had histologically immature tubules, being consistent with the previous reports [3, 22]. 2) Moreover, the histological findings on the ureter of affected side showed the discontinuous lacunae, reflecting the immature stage. 3) The ureteral lumen was not patent to the bladder.

Basically the dialysis kidney becomes atrophic at the end stage. As McManus and Hughson [13] reported, the minimum weight of dialysis kidneys was around 20 g in 2 cases out of 42. However, the present case weighed only 9 g, a value suggesting developmental abnormality rather than atrophic reduction from a once-fully developed kidney. From histopathological standpoint, this case was completely devoid of renal glomeruli, being consistent with incomplete development of the nephrons. Furthermore, the renal tissue contained undifferentiated renal convoluted tubules [7] that resembled collecting ducts, and various-sized developing renal tubules, which were similar to embryonic hyperplasia reported in previous studies [3, 22]. Immunohistochemical staining of these structures with anti-cytokeratin (1, 5, 10, 14) and anti-h-caldesmon antibodies revealed epithelial cells surrounded by smooth muscle cells. These muscle cells were positive for αSMA immunoreactivity, which is usually expressed in the vascular smooth muscle cells, myoepithelial cells, pericytes, and prospective cardiomyocytes during the early cardiogenesis [12]. In the present case, these αSMA-positive cells were likely to be myofibroblasts that proliferated in the interstitium secondary to the abnormal interaction taking place between the metanephric blastema and ureteric buds. On this account, the concentric proliferation of interstitium in the left kidney is considered to be the immature mesenchymal cells rather than the inflammatory cells. As for evidence supporting this claim, the left renal tissue did not show any sign of inflammation. These findings collectively support the idea that the present case matches the criteria of previous reports by Ashley and Mostofi [3] and Woolf *et al.* [22], who described the dysplastic kidneys, and those of Potter's cystic kidney type II [17].

The ureteric bud derived from the mesonephric duct (Wolffian duct) during the 4th week of gestation plays an important role in nephrogenesis. On day 35, the ureteric bud forms a lumen lined with cuboidal epithelium, followed by extensive proliferation of epithelia to fill the lumen along the entire length of the ureteral anlagen on day 37. On day 40, the recanalization process commences at the middle portion. Finally, it rapidly extends in both the proximal and distal directions, completing the recanalization of the ureter [11, 18]. The same processes were observed in rats and mice [1, 2, 10]. Taking these processes into account, the failure of ureteral recanalization leads to incomplete interaction of the ureteric bud with the metanephric blastema during early phase of development. In fact, a part of the renal mesenchyme commences to develop the glomeruli by forming lacunae under the influence of the ureteral bud. In this sense, the complete absence of renal glomeruli in the present case should be considered to be due to congenital etiology.

Recently, several genetic analyses of the EMT for the development of ureter have been published [1]. For example, glial-derived neurotropic factor (GDNF) released from the metanephric blastoma induced the ureter budding from the mesonephric duct [8, 16]. Loss of interaction by abolishing GDNF signaling pathway either disrupts or deteriorates the budding and outgrowth of ureter, leading to agnesis, hypoplasia or dysplasia of kidney and ureter [1]. Concerning the recanalization process, similar mechanisms are proposed and partly verified in the duodenum, where the involvement of Fgf10 has been documented [9], although there is no relevant reference on a similar process for the ureter.

In summary, the present case showed congenital renal and ureteral dysplasia and may help to further clarify the histogenesis of congenital renal anomalies.

V. Acknowledgments

We thank K. Sawa-Nobori (Department of Anatomy and Cell Biology, University of Yamanashi) for her secretarial and technical assistance, and M. Yoda and Y. Koshimizu (Department of Human Pathology, University of Yamanashi) for their technical assistance. We wish to express our gratitude to Dr. Mitsui at the Kofu Kyoritsu Hospital for providing us with clinical data. This study was partly supported by the Strategic Project for Promotion of Science and Education from the University of Yamanashi to ST, and Grants-in-Aid for Encouragement of Scientists from MEXT to HF.

VI. References

1. Airik, R. and Kispert, A. (2007) Down the tube of obstructive nephropathies: The importance of tissue interactions during ureter development. *Kidney Int.* 72; 1459–1467.
2. Alcaraz, A., Vinaixa, F., Tejedo-Mateu, A., Fores, M. M., Gotzens, V., Mestres, C. A., Oliveira, J. and Carretero, P. (1991) Obstruction and recanalization of the ureter during embryonic development. *J. Urol.* 145; 410–416.
3. Ashley, D. J. and Mostofi, F. K. (1960) Renal agenesis and dysgenesis. *J. Urol.* 83; 211–230.
4. Burns, W. C., Kantharidis, P. and Thomas, M. C. (2007) The role of tubular epithelial-mesenchymal transition in progressive kidney disease. *Cells Tissues Organs* 185; 222–231.
5. Hay, E. D. and Zuk, A. (1995) Transformations between epithelium and mesenchyme: normal, pathological, and experimentally induced. *Am. J. Kidney Dis.* 26; 678–690.
6. Hughson, M. D., McManus, J. F. A. and Hennigar, G. R. (1978) Studies on "End-stage" kidneys. II. Embryonal hyperplasia of Bowman's capsular epithelium. *Am. J. Pathol.* 1; 71–84.
7. Itatani, H., Koide, T., Okuyama, A., Takeuchi, M. and Sonoda, T. (1976) Maldeveloped kidney: Its classification and the time of onset. *Nihon hinyouki gakkai zasshi* 67; 178–187 (in Japanese).
8. Jijiwa, M., Fukuda, T., Kawai, K., Nakamura, A., Kurokawa, K., Murakumo, Y., Ichihara, M. and Takahashi, M. (2004) A targeting mutation of tyrosine 1062 in Ret causes a marked decrease of enteric neurons and renal hypoplasia. *Mol. Cell. Biol.* 24; 8026–8036.
9. Kanard, R. C., Fairbanks, T. J., De Langhe, S. P., Sala, F. G., Del Moral, P. M., Lopez, C. A., Warburton, D., Anderson, K. D., Bellusci, S. and Burns, R. C. (2005) Fibroblast growth factor-10 serves a regulatory role in duodenal development. *J. Pediatr. Surg.* 40; 313–316.
10. Leeson, T. S. and Leeson, C. R. (1965) The ureter. Fine structure changes during its development. *Acta Anat.* 62; 60–79.
11. Maizels, M. (1986) Normal development of the urinary tract. In "Campell's Urology", ed. by P. C. Walsh and R. F. Gittes, WB Saunders, New York, pp. 1638–1664.
12. Matsui, H., Sakabe, M., Sakata, H., Nakatani, K., Ikeda, K., Fukui, M., Ando, K., Yamagishi, T. and Nakajima, Y. (2006) Heart myofibrillogenesis occurs in isolated chick posterior blastoderm: A culture model. *Acta Histochem. Cytochem.* 39; 139–144.
13. McManus, J. F. A. and Hughson, M. D. (1979) Histopathology of arteries and veins in the end-stage/dialysis kidney. *Pathol. Annu.* 14pt2; 23–59.
14. McManus, J. F. A., Michael, M. D. and Hughson, M. D. (1979) New therapies and new pathologies. End-stage-dialysis kidneys. *Arch. Pathol. Lab. Med.* 103; 53–57.
15. Ng, Y. Y., Huang, T. P., Yang, W. C., Chen, Z. P., Yang, A. H., Mu, W., Nikolic-Paterson, D. J., Atkins, R. C. and Lan, H. Y. (1998) Tubular epithelial-myofibroblast transdifferentiation in progressive tubulointerstitial fibrosis in 5/6 nephrectomized rats. *Kidney Int.* 54; 864–876.
16. Pepicelli, C. V., Kispert, A., Rowitch, D. H. and McMahon, A. P. (1997) GDNF induces branching and increased cell proliferation in the ureter of the mouse. *Dev. Biol.* 192; 193–198.
17. Potter, E. L. (1972) Normal and Abnormal Development of the Kidney. Year Book Medical Publishers Inc., Chicago, pp. 105–107, 154–181.
18. Ruano-Gill, D., Coca-Payeras, A. and Tejedo-Mateu, A. (1975) Obstruction and normal recanalization of the ureter in the human embryo. Its relation to congenital ureteric obstruction. *Eur. Urol.* 1; 287–293.
19. Sakaguchi, H. (1996) Development of kidney, congenital anomaly of kidney. In "Current Encyclopedia of Pathology: Kidney 1", ed. by S. Iijima, Nakayama Shoten, Tokyo, 15A, pp. 71–93 (in Japanese).
20. Schedl, A. (2007) Renal abnormalities and their developmental origin. *Nature Reviews/Genetics* 8; 791–802.
21. Siloniz, C. and Riera, A. A. (1894) Nuevo Tratado de Anatomía Descriptiva y Embriología. Barcelona, Imprenta Subirana, Tomo II, pp. 389–408. (in Spanish)
22. Woolf, A. S., Price, K. L., Scambler, P. J. and Winyard, P. J. D. (2004) Evolving concepts in human renal dysplasia. J. Am. Soc. Nephrol. 15; 998–1007.